



New doping process mode to synthesize in situ N-MWNTs in novel coaxial nanostructure



O. Guellati^{a,b,c,*}, F. Antoni^d, M. Guerioune^a, D. Bégin^{b,**}

^a Laboratoire d'Etude et de Recherche des Etats Condensés (LEREC), Département de Physique, Université Badji-Mokhtar de Annaba, BP 12, 23000 Annaba, Algeria

^b Institut de Chimie et Procédés pour l'Energie, l'Environnement et la Santé (ICPEES) – ECPM – CNRS – Uds, 25 rue Becquerel, 67087 Strasbourg Cedex 2, France

^c Univ Souk-Ahras, Fac. Sci, BP 1553, 41000 Souk-Ahras, Algeria

^d Laboratoire ICube – DESSP (UMR7357 CNRS/Uds), 23 Rue du Loess – BP20, 67037 Strasbourg Cedex 02, France

ARTICLE INFO

Keywords:

Nitrogen-doped MWNT
Catalytic CVD in situ growth
Functionalization
Doping
Coaxial nanostructures
XPS spectroscopy

ABSTRACT

Nitrogen-doped MWNT “N-MWNT” have gained an increasing interest because particularly of their electronic properties allowing their use in specific applications such as catalysis, sensors, nano-electronics and energy storage.

In this investigation, novel coaxial structures consisting of concentric shells of pure carbon MWNT cores with external nitrogen-doped carbon walls (N-MWNT) were produced using a catalytic CVD process, with ethane and ammonia as carbon and nitrogen sources over Fe–Al₂O₃ support. In order to optimize the growth conditions of such N-MWNT nanostructures, we investigate the influence of different key parameters, i.e., ammonia injection moment in two doping process modes “Instantaneously doping and Mid-doping”, growth temperature (750 and 850 °C) and the presence of H₂ as reducer gas in the reaction environment. A strong correlation between ammonia injection duration (60, 90 and 120 min) and nitrogen content (from 0.4 at.% to 2.2 at.%) incorporated in the nanotube products was observed and different coordination between C and/or O atoms have been described by XPS. These functionalized MWNTs were characterized using HR-TEM, FESEM, XPS, BET, TG analyses and Raman spectroscopy in order to determine their structural characteristics (graphitization and crystallinity) in quantitative and qualitative ways.

1. Introduction

The doping of carbon nanotubes (CNT) with heteroatoms [1] has been frequently used to enhance or tune their physicochemical properties. Thus, it allows modifying the electronic properties of the tubes by replacing carbon by dopant atoms containing additional electrons (donors) or fewer valence electrons (acceptors), similar to the techniques used in the semiconductor industry. Among the dopants, nitrogen has a particular interest in modifying the electronic properties of CNT or other carbonaceous materials [2–4]. The enhancement of other N-CNT properties, including the chemical reactivity [5], the dispersity in a variety of solvents/matrices [6], the structural strength [7] or the thermal conductivity [8] has been also reported. Indeed, extrinsic or intrinsic doping of nanotube surfaces as a functionalization process can lead to localized electronic states in different coordination kinds [9–11]. For this reason, extrinsically doped CNT should be excellent candidates for a new generation of controlled chemically functionalized

NT materials for different fields, such as catalysis, sensors, nano-electronics, field emission, Li-ion storage, polymer-CNT composites, etc. [5,6,8,12,13]. The literature survey shows that the N-doping of CNT usually induced lattice deformations, i.e., the formation of regular and irregular compartments that replace or accompany the multi-walled structure [9,12,14,15]. Those defects, e.g., ‘bamboo’ and/or ‘nanobell’-morphologies could translate further into twists and corrugations. In addition, the incorporation of nitrogen was found to be the driving force in the formation of defect sites in the carbon sp²-network. Therefore, a facile and low-cost synthetic route to create 2D and 3D nanotube junctions (using SWNTs or MWNTs) is inevitably required, as several authors have pointed out [14,16].

In this paper, our aim is to report a scale-able catalytic-CVD synthesis in order to obtain new nanostructure forms of N-MWNT with a high yield, a high purity and crystallinity. We compare the effect of two different doping modes, under two growth temperatures (with and without H₂ as etching gas). We particularly present in this investigation

* Corresponding author at: Laboratoire d'Etude et de Recherche des Etats Condensés (LEREC), Département de Physique, Université Badji-Mokhtar de Annaba, BP 12, 23000 Annaba, Algeria.

** Corresponding author.

E-mail addresses: guellati23@yahoo.fr (O. Guellati), dominique.begin@unistra.fr (D. Bégin).

<http://dx.doi.org/10.1016/j.cattod.2017.03.041>

Received 29 December 2016; Received in revised form 16 March 2017; Accepted 24 March 2017

Available online 10 April 2017

0920-5861/ © 2017 Elsevier B.V. All rights reserved.

Table 1
Different characteristics of the synthesized MWNT in the total (full doping) or partial (mid-doping) presence of NH_3 .

	NH_3 (duration)	T ($^\circ\text{C}$)	m_{dep} ($\text{g}_{\text{NWC}}/\text{g}_{\text{cat}}$)	S_{BET} (m^2/g)	e_{dop} (nm)
Without doping	150 min	750	4.4	130	0
	180 min	750	5.7	140	0
Mid-doping	60–60 min	750	3.6	198	4
		850	1.8	53	8
		850 (+ H_2)	1.2	82	10
	90–90 min	750	4.4	160	3
		850	2.8	24	14
		850 (+ H_2)	1.2	87	–
Full doping	120 min	750	2.4	214	–
		850	1.6	80	–
		850 (+ H_2)	1.2	87	–

e_{dop} : thickness of waved walls, m_{dep} : weight of N-MWNT/weight of catalyst.

Table 2
Microraman D and G band peak characteristics of the synthesized N-MWNT depending of the doping mode.

		G_{Position}	D_{Position}	$I_{\text{D}}/I_{\text{G}}$	N/C (at.%)
Without NH_3 750 $^\circ\text{C}$	150	1598	1331	1.04	0
	180	1598	1328	1.05	0
60/60	750	1587	1333	1.01	0.4
	850	1581	1335	0.86	1.6
	+ H_2	1577	1327	0.79	1.2
90/90	750	1580	1324	0.99	0.7
	850	1586	1331	0.87	1.0
120	750	1595	1319	1.1	1.4
	850	1589	1321	1.07	2.0
	+ H_2	1598	1331	1.03	2.2

an original doping process (partial doping or Mid-doping) to introduce in situ functional N groups on the surface of the MWCNT by a classical CVD method: in a first time no NH_3 is present in the reactant, and then NH_3 is introduced during the synthesis.

2. Experimental procedure

MWNT containing substitutionally “doped” nitrogen were synthesized over Fe- Al_2O_3 support as described elsewhere [6,12] using atmospheric pressure catalytic-CVD technique (CCVD) [17,18]. Thus, the N-MWNT synthesis was performed from the decomposition of $50 \text{ cm}^3/\text{min}$ C_2H_6 and $50 \text{ cm}^3/\text{min}$ NH_3 at 750 and 850 $^\circ\text{C}$ with (or without) $100 \text{ cm}^3/\text{min}$ of H_2 as etching gas in quartz reactor (with 1000:70:2 mm dimension).

In this investigation, “Continuous or instantaneously” doping was performed in the presence of NH_3 during all the MWNT synthesis duration, while we call “Mid doping” which consists in the synthesis of MWNT firstly without NH_3 followed by a CCVD growth in the presence of NH_3 (the half remaining reaction duration). After, the crude doped products were purified in two steps using basic (NaOH) and acidic treatments (HCl/ HNO_3) under reflux in order to remove the alumina support and the residual iron catalyst [12,19].

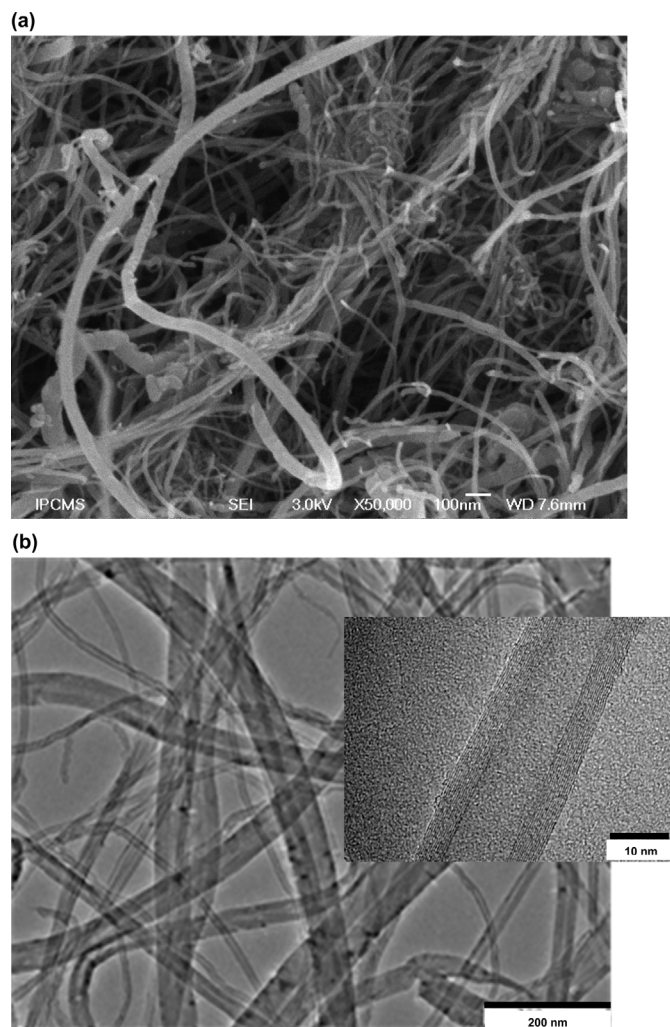


Fig. 1. FESEM (a) and high-resolution TEM (b) micrographs of un-doped MWNT synthesized with catalytic CVD at 850 $^\circ\text{C}$ during 2 h.

N-MWNT were characterized using FESEM (JEOL 6700-FEG microscope) and HR-TEM (JEOL 2100F) working under an accelerated voltage of 200 kV with a point-to-point resolution of 0.23 nm in order to control the quality, structure and overall morphology of the produced MWNTs. XPS analyses were performed with a MULTILAB 2000 (THERMO) spectrometer equipped with Al $K\alpha$ anode ($h\nu = 1486.6 \text{ eV}$) during 10 min of acquisition in order to achieve a good signal-to-noise ratio. XPS peak deconvolutions were made with the “Avantage” software from Thermoelectron Company. The C_{1s} photoelectron binding energy was set at $284.6 \pm 0.2 \text{ eV}$ relatively to the Fermi level and used as reference for calibrating the other peak positions. XPS was used to examine the chemical composition of functional groups and their concentration in different bonding. Raman spectroscopy was carried out on a Horiba Jobin Yvon LabRAM Aramis confocal spectrometer (with a spot size of $0.4 \mu\text{m}^2$ and 1 cm^{-1} resolution) working with a 532 nm wavelength. All spectra show mainly two bands: $\sim 1350 \text{ cm}^{-1}$ (D band) and $\sim 1576 \text{ cm}^{-1}$ (G band). The G band originates from the Raman active E_{2g} mode explaining the in-plane atomic displacements, otherwise, the origin of D band explains the disorder features. The D/G peak intensity ratio was studied in order to determine the “defective to graphitic” carbon ratio

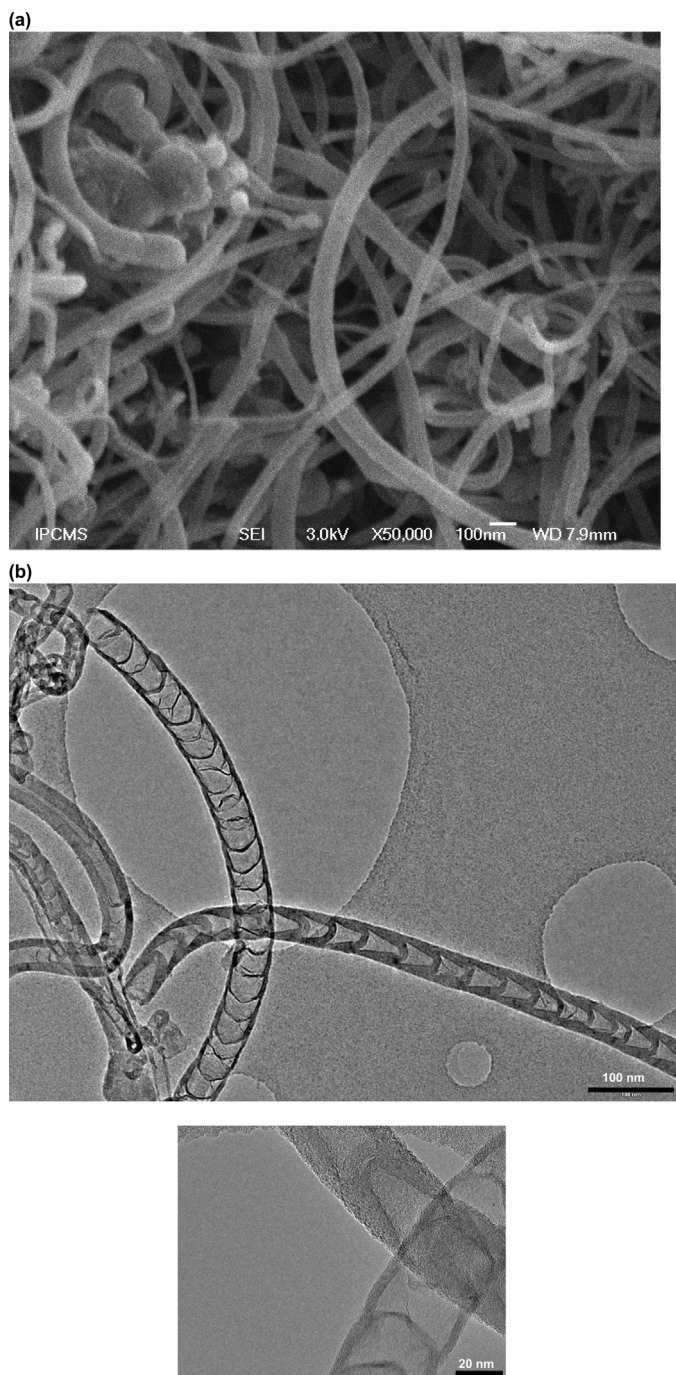


Fig. 2. FESEM (a) and High-resolution TEM (b) micrographs of N full doped MWNT (bamboo shape-like N-MWNT) synthesized with catalytic CVD at 850 °C during 2 h.

present inside the synthesized N-MWNTs. TG analyses were carried out in a Q5000 apparatus (TA instrument) under 20 sccm air flow. The temperature was increased from room temperature to 1000 °C with a heating rate of 10 °C/min. Specific surface area measurements were

carried out with a Tristar (Micromeritics) sorptometer using nitrogen as adsorbent at liquid nitrogen temperature. Before the measurements, the samples were already out-gassed at 300 °C during 5 h in order to desorb impurities and moisture from its surface.

3. Results and discussion

Different characteristics of the synthesized N-MWNT in the total (full doping) or partial (mid-doping) presence of NH_3 during the growth are gathered in Table 1. If we consider the yield in MWNT as a function of the temperature, the higher the temperature, the lower the yield for both doping modes (the yield corresponds to the ratio deposited carbon/catalyst amount). Besides, the nitrogen content in the obtained nanotubes, ranged from 0 to 3 at.% (see later in Table 2): it was directly correlated to the concentration of NH_3 in the precursor mixture. Furthermore, it is well known that the growth of CNT in the presence of NH_3 is generally characterized by a lower yield in carbon which is confirmed by the mid-doping: in such a process; however, in this case, the first part of the synthesis is performed without NH_3 with a higher yield so that the total amount of CNT at the end of the reaction is higher (for an equivalent synthesis time).

Consequently, as revealed by Raman spectroscopy, the incorporation of nitrogen atoms into the nanotube walls was found to be proportional to the defect identification ratio as well as the deformed walls thickness. From a quantitative point of view, the N/C atomic ratio has been determined by XPS measurements. We will see that the higher the temperature, the higher the N/C ratio, showing that the incorporation of nitrogen in the graphitic lattice needs higher temperatures. In the case of the full doping mode, the N content is higher: it has been shown that the incorporation of N in the carbonaceous structure is favored in the internal bridges [15] (in the case of the bamboo like structures), that cannot be observed in the case of the partial doping for which N is only incorporated on the external walls. Typical pictures of MWNTs samples can be seen in Fig. 1 and sometimes, bamboo-like structures obtained in the presence of nitrogen can also be seen (Fig. 2).

These high resolution micrographs clearly show that, to the best of our knowledge, it is the first report on the production of coaxial nanocables composed of an internal core of pure carbon MWNTs and an external concentric N-doped carbon shell as shown by the FESEM pictures in Fig. 3 and TEM micrographs in Fig. 4.

So, we note that this proposed way is one of the first approaches to actually exploit the chemistry of the N-doped CNTs in order to create new nanostructured N-MWNT, conversely to those obtained by Lepro et al. [16] using another method: in this case, they observed an increase of the electrical conductivity due to the injection of electronic states in the graphene sheet by the nitrogen atoms. More recently, Purceno et al. [20] observed another mechanism: in the presence or not of acetonitrile in the gas flow: without acetonitrile, a typical CNT growth is observed, and when acetonitrile is added in the gas flow, they observe the growth of bamboo-like structures (which are more hydrophobic) in the extension of the initial CNTs.

We also emphasize that these coaxial hetero-structures have not been theoretically proposed, and this account demonstrates an easy way to synthesize such new nanostructures, and opens up new perspectives to the study of the controlled growth of coaxial nanotubes and junctions.

If we consider the mid-doping (doping process mode up to now never described in the literature), the result is rather surprising: the presence of bamboo-like structures is very low and during the growth phase in the presence of NH_3 , some additional walls (called waved walls because they are not in parallel form) covering the CNTs can be observed (see Fig. 4b and d). The thickness of such waved walls

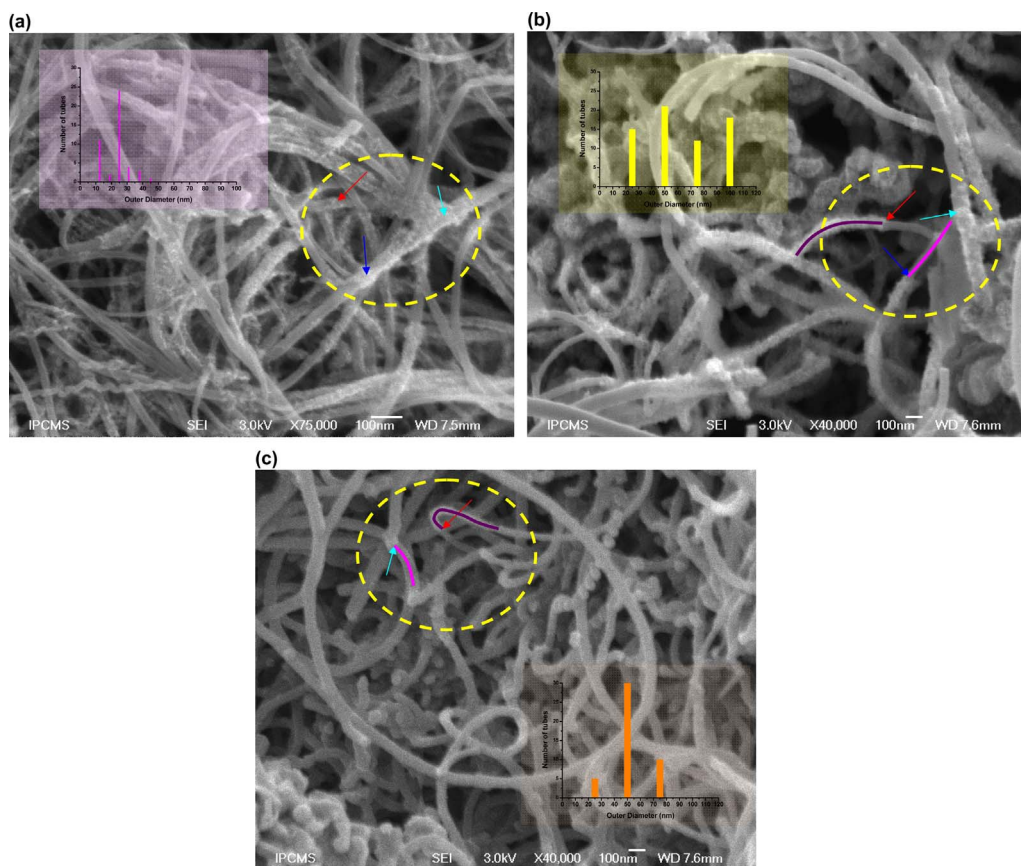


Fig. 3. FESEM micrographs of N mi-doped MWNT (N-MWNT nano hybrid structure) synthesized with catalytic CVD at 750 °C – 60 min without NH₃ then 60 min in the presence of NH₃ (a), 850 °C – 60 min without NH₃ then 60 min in the presence of NH₃ (b) and 850 °C – 90 min without NH₃/then 90 min in the presence of NH₃ (c). Yellow circle and arrows represent the doping layer. (For interpretation of the references to color in this figure legend, the reader is referred to the web version of this article.)

depends of the synthesis temperature and the NH₃ duration, as can be seen in Table 1, and it is comprised between 3 and 14 nm (measured on HRTEM images). Thus, nitrogen is incorporated in these walls and we can observe that the N/C ratio rises with the increasing growth temperature.

TGA measurements have shown that in the presence of nitrogen groups, N-MWNT burn at a temperature lower than that of pure MWNT (by a typical value of 50 °C) as shown in Fig. 5. Generally, in a “classical” growth without NH₃, the higher the CNT synthesis temperature, the higher their thermal stability. However, in the presence of NH₃, as the ratio N/C increases with the synthesis temperature, their thermal stability decreases by increasing the synthesis temperature.

In Fig. 6, we can observe the typical D and G bands of the MWNT obtained after the two doping modes: in all cases, as expected, the higher the synthesis temperature, the lower the I_D/I_G ratio (see Table 2) as well as the peaks shifting: that shows a higher graphitization rate [21]. This rate is also increased in the presence of H₂: indeed, H₂ is well known to avoid the amorphous carbon formation during the growth process which enhances the N-MWNT yield and their crystallinity rate [22]. Such a ratio is, of course, always lower in the case of mid-doping in comparison to the full doping case.

Specific surface area (Table 1) shows also the great importance of the synthesis temperature as well as the doping duration. A strong decrease of this specific area is systematically observed when the

temperature increases from 750 °C to 850 °C. The Raman observations as well as TG analysis results show also an increase of the degree of graphitization (decrease of the I_D/I_G ratio and shift of the oxidation temperature to higher values)

In Fig. 7 are represented the N_{1s}-XPS spectrum contributions. Five kind of bonds have been identified including three distinct features: pyridine “N_P”, pyrrole “N_{pyr}” (and/or pyridone) and quaternary “N_Q” obtained, respectively, around 398, 400 and 401 eV according to the literature [3,11].

We can also see that, when the temperature of the synthesis increases (b and c) in the case of the bamboo-like structures, the contribution of quaternary “N_Q” is more important attesting of a higher graphitization degree (same observation in the case of the mid-doping at 850 °C). Indeed, in the case of a post treatment of carbonaceous materials in the presence of nitrogen based precursors, most of the additional groups are generally pyrrolic or pyridonic while N–X bonds are not negligible. This is very unfavorable for the transport properties of such materials for instance. Moreover, the presence of oxygen groups, which are certainly due to the washing of the N-MWNTs with a strong and oxidant acid in the purification step, can mainly be seen at 399 and 405 eV corresponding, respectively, to pyrrolic or pyridonic and oxidized nitrogen (N–O).

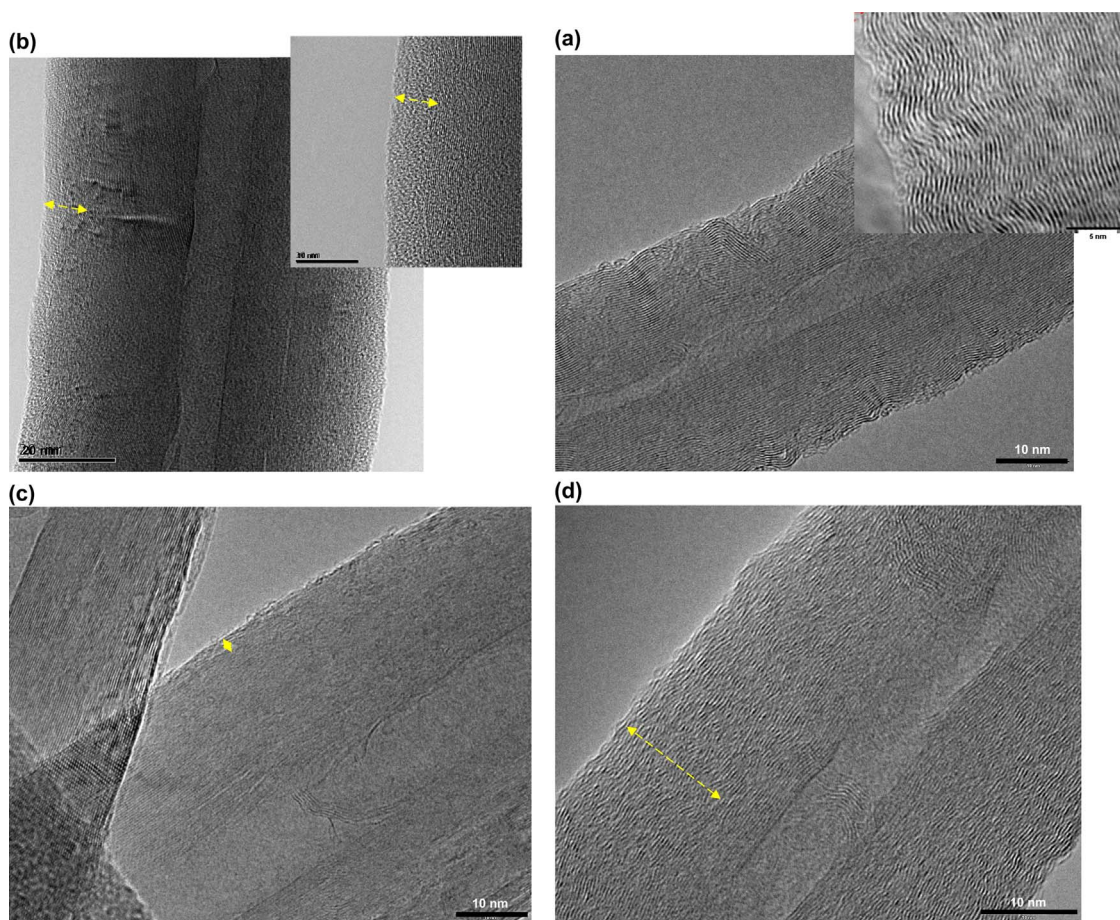


Fig. 4. HRTEM micrographs of N mid-doped MWNT obtained at 750 °C, (a, c) for a synthesis of 60 min without NH₃ then 60 min in the presence of NH₃ and 850 °C (b, d) for a synthesis of 90 min without NH₃ then 90 min in the presence of NH₃. Yellow circle and arrows represent the doping layer. (For interpretation of the references to color in this figure legend, the reader is referred to the web version of this article.)

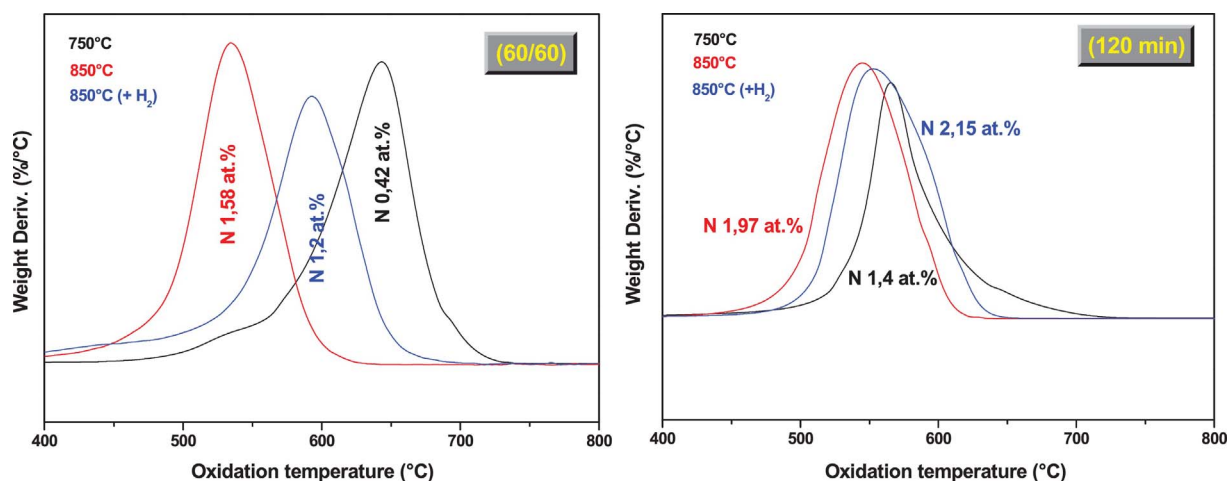


Fig. 5. Effect of the doping mode: mi-doping (60/60) and full doping (120 min) as well as the H₂ presence at two different growth temperatures on the oxidation resistance of purified MWNTs.

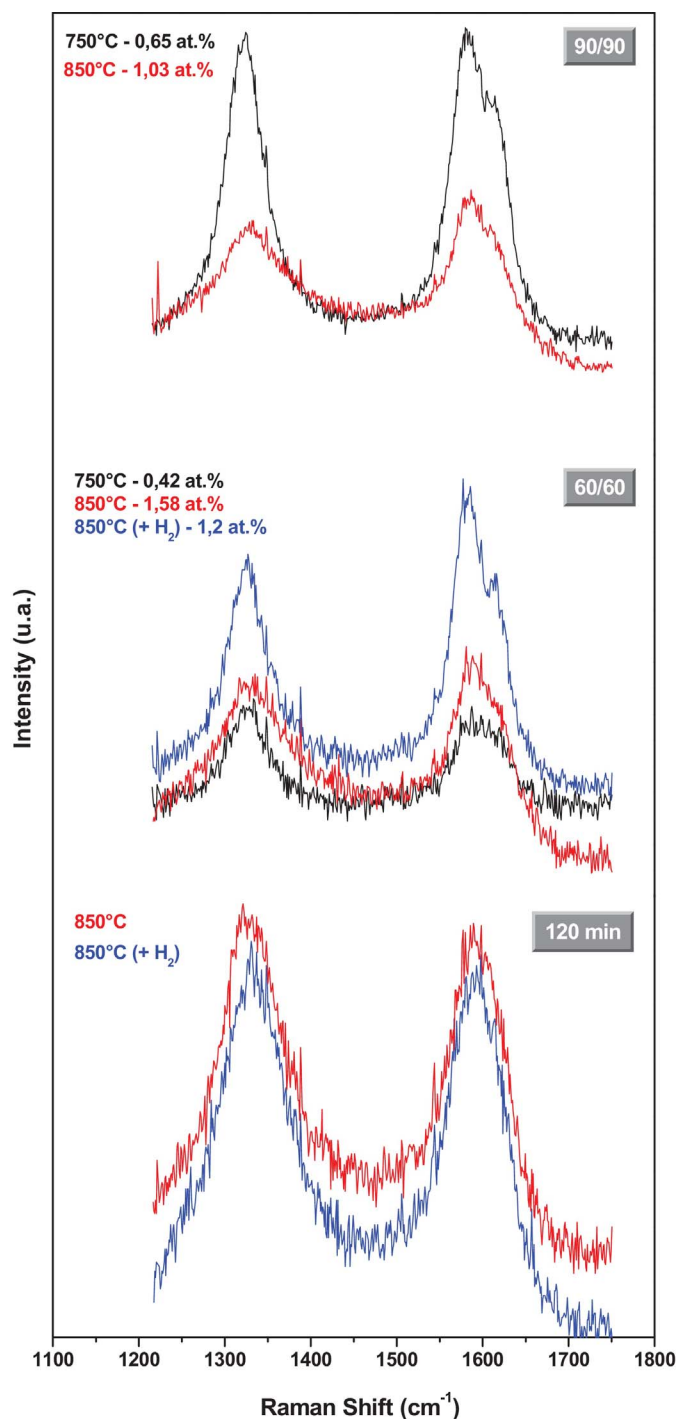


Fig. 6. D and G Raman peak features as a function of the doping mode.

4. Conclusion

A one-step process, using ammonia as nitrogen doping source, was successfully used to produce new nanostructures of N doped MWNT in nanohybrid coaxial form (MWNTs@N-MWNTs). This result presents an important focus of current research especially for future applications. Our original results with this new doping way show that the partial N-doping is a promising way to control the structure of MWNT.

Consequently, we have shown that this doping mode allows obtaining nano-hybrid MWNT@N-MWNT and/or bamboo shape-like N-MWNT depending to the ammonia injection moment and duration. The “Mid-doping” is a very original method, because it avoids (strongly decreased) the bamboo-like structure formation and allows obtaining CNTs with nitrogen on their surface strongly linked to carbon atoms (in pyridinic and quaternary coordinations), which is impossible to obtain with a classical post treatment of CNT. Moreover, this process provides

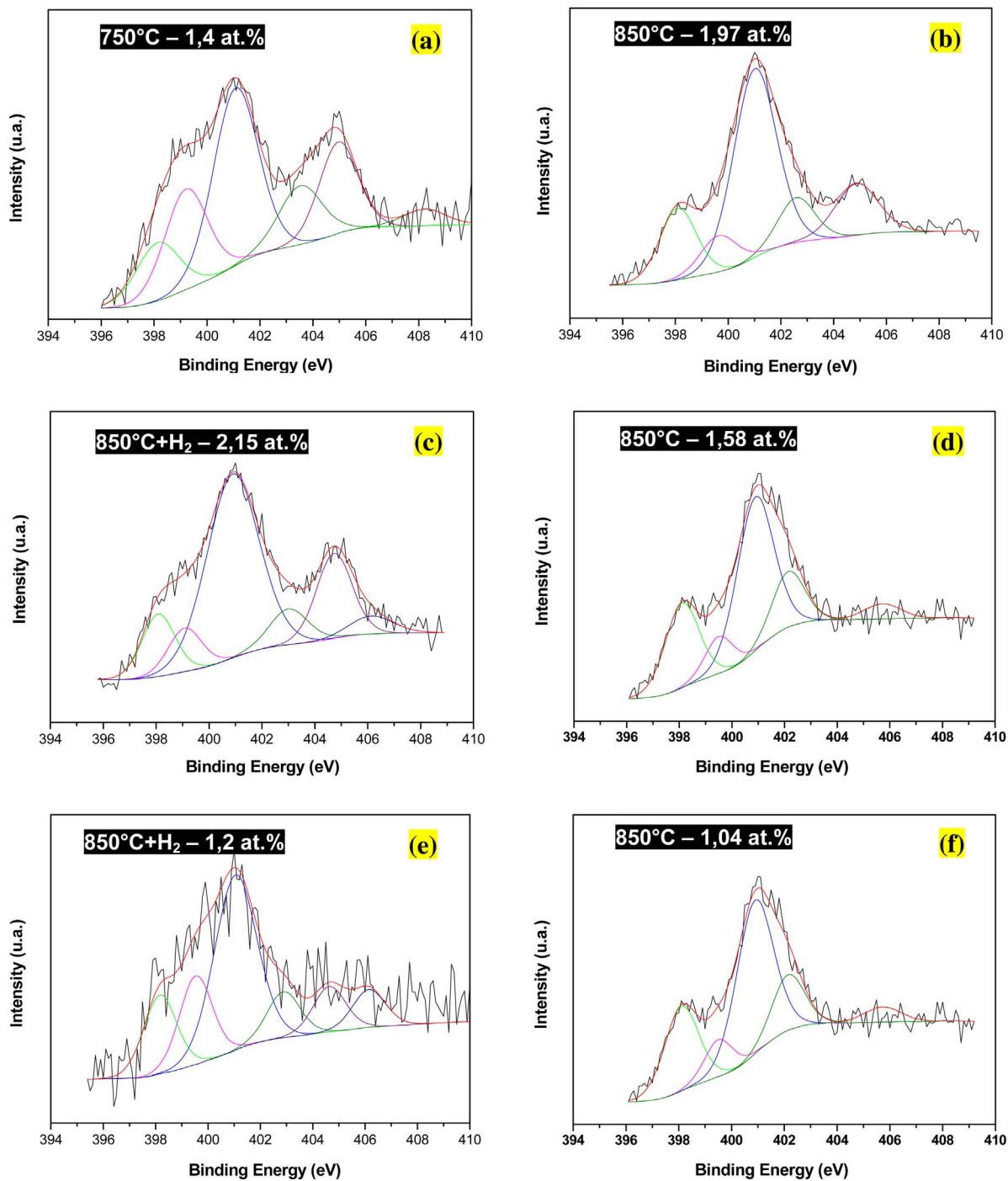


Fig. 7. “N_{1s}” XPS spectra of bamboo shape-like CNT (full doping – a–c) and “nano-hybrid” CNT (mid-doping for a synthesis of 60 min without NH₃ then 60 min in the presence of NH₃ – d, and for a synthesis of 90 min without NH₃ then 90 min in the presence of NH₃ – e.

a new way to ‘activate’ some regions along the tube external walls. Furthermore, the H₂ presence in the reactant avoids the amorphous carbon formation which enhanced the N-MWNT yield and the crystallinity rate.

Finally, the N-MWNT in this novel form can be good potential candidates for various applications such as catalysis, nanoelectronics, energy storage, etc. where the role of the active metallic phase can be replaced by such metal free N-MWNT.

Acknowledgement

The present work has been financially supported by the doctoral scholarship grant of the Algerian-MHESR. The authors would like to acknowledge Th. Romero (LMSPC), D. Ihiwakrim (IPCMS), P. Bernhardt (LMSPC) for performing, respectively, FESEM, HR-TEM, and XPS experiments.

References

- [1] M. Glerup, V. Krstić, C. Ewels, M. Holzinger, G. Van Lier, *Doped Nanomaterials and Nanodevices*, Ed. Wei Chen. ASP, 2008 ISBN: 1-58883-110-8.
- [2] C. Tuci, C. Zafferoni, P. D'Ambrosio, S. Caporali, M. Ceppatelli, A. Rossin, T. Tsoufis, M. Innocenti, G. Giambastiani, Tailoring carbon nanotube N-dopants while designing metal-free electrocatalysts for the oxygen reduction reaction in alkaline medium, *ACS Catal.* 3 (2014) 2108–2111.
- [3] C. Ewels, M. Glerup, V. Krstić, *Chemistry of Carbon Nanotubes*, in: V.A. Basiuk, E.V. Basiuk (Eds.), American Scientific Publishers, 2008 ISBN 1-58883-129-9.
- [4] B. Grzyb, C. Hildenbrand, S. Berthon-Fabry, D. Bégin, N. Job, A. Rigacci, P. Achard, Functionalisation and chemical characterisation of cellulose-derived carbon aerogels, *Carbon* 48 (2010) 2297–2307.
- [5] L.F. Mabena, S.S. Ray, S.D. Mhlanga, N.J. Coville, Nitrogen-doped carbon nanotubes as a metal catalyst support, *Appl. Nanosci.* 1 (2011) 67–77.
- [6] J. Amadou, K. Chizari, M. Houllé, I. Janowska, O. Ersen, D. Bégin, C. Pham-Huu, N-doped carbon nanotubes for liquid-phase C=C bond hydrogenation, *Catal. Today* 138 (2008) 62–68.
- [7] T.Y. Kim, K.R. Lee, K.Y. Eun, K.H. Oh, Carbon nanotube growth enhanced by nitrogen incorporation, *Chem. Phys. Lett.* 372 (2003) 603–607.
- [8] S. Van Dommele, K.P. de Jong, J.H. Bitter, Nitrogen-containing carbon nanotubes as solid base catalysts, *Chem. Commun.* 46 (2006) 4859–4861.
- [9] J.W. Jang, C.E. Lee, S.C. Lyu, T.J. Lee, C.J. Lee, Structural study of nitrogen-doping effects in bamboo-shaped multi-walled carbon nanotubes, *Appl. Phys. Lett.* 84 (2004) 2877–2879.
- [10] B.G. Sumpter, V. Meunier, J.M. Romo-Herrera, E. Cruz-Silva, D.A. Cullen, H. Terrones, Nitrogen-mediated carbon nanotube growth: diameter reduction, metallicity, bundle dispersability, and bamboo-like structure formation, *ACS Nano* 1 (2007) 369–375.
- [11] O. Guellati, Ph.D. thesis, Annaba, Algeria, 2013.
- [12] K. Chizari, A. Deneuve, O. Ersen, I. Florea, Y. Liu, D. Edouard, I. Janowska, D. Bégin, C. Pham-Huu, Nitrogen-doped carbon nanotubes as a highly active metal-free catalyst for selective oxidation, *ChemSusChem* 5 (2012) 102–108.
- [13] D.S. Su, J. Zhang, B. Frank, A. Thomas, X. Wang, J. Paraknowitsch, R. Schlög, Metal-free heterogeneous catalysis for sustainable chemistry, *ChemSusChem* 3 (2010) 169–180.
- [14] H. Ba, J.J. Luo, Y. Liu, D.V. Cuong, G. Tuci, G. Giambastiani, J.M. Nhut, N.D. Lam, O. Ersen, D.S. Su, C. Pham-Huu, Macroscopically shaped monolith of nanodiamonds @ nitrogen-enriched mesoporous carbon decorated SiC as a superior metal-free catalyst for the styrene production, *Appl. Catal. B: Environ.* 200 (2017) 343–350.
- [15] I. Florea, O. Ersen, R. Arenal, D. Ihiwakrim, C. Messaoudi, K. Chizari, I. Janowska, C. Pham-Huu, 3D analysis of the morphology and spatial distribution of nitrogen in nitrogen-doped carbon nanotubes by energy-filtered transmission electron microscopy tomography, *J. Am. Chem. Soc.* 134 (2012) 9672–9680.
- [16] X. Lepro, Y. Vega-Cantu, F.J. Rodriguez-Macias, Y. Bando, D. Golberg, M. Terrones, Production and characterization of coaxial nanotube junctions and networks of CNx/CNT, *Nano Lett.* 7 (8) (2007) 2220–2226.
- [17] G. Gulino, R. Vieira, J. Amadou, P. Nguyen, M.J. Ledoux, S. Galvagno, G. Centi, C. Pham-Huu, C₂H₆ as an active carbon source for a large scale synthesis of carbon nanotubes by chemical vapour deposition, *Appl. Catal. A: Gen.* 279 (2005) 89–97.
- [18] M.G. Donato, S. Galvano, M. Lanza, G. Messina, E. Piperoulos, A. Pistoni, S. Santagelo, Influence of carbon source and Fe catalyst support on growth of multi-walled carbon nanotubes, *J. Nanosci. Nanotechnol.* 9 (2009) 3815–3823.
- [19] J. Amadou, D. Bégin, P. Nguyen, J.P. Tessonnier, T. Dintzer, E. Vanhaecke, M.J. Ledoux, C. Pham-Huu, Synthesis of a carbon nanotube monolith with controlled macroscopic shape, *Carbon* 44 (2006) 2587–2589.
- [20] A.D. Purceno, B.F. Machado, A.P.C. Tixeira, T.V. Medeiros, A. Benyounes, J. Beausoleil, H.C. ezezes, Z.L. Cardeal, R.M. Lago, P. Serp, Magnetic amphiphilic hybrid carbon nanotubes containing N-doped and undoped sections: powerful tensioactive nanostructures, *Nanoscale* 7 (2015) 294–300.
- [21] A.C. Ferrari, J. Robertson, Interpretation of Raman spectra of disordered and amorphous carbon, *Phys. Rev. B* 61 (2000) 14095–14107.
- [22] W. Wasel, K. Kuwana, P.T.A. Reilly, K. Saito, Experimental characterization of the role of hydrogen in CVD synthesis of MWCNT, *Carbon* 5 (2007) 833–838.